Available online at www.sciencedirect.com
SCIENCE DIRECT®
International Journal of Solids and Structures 41 (2004) 7309–7328
INTERNATIONAL JOURNAL OF SOLIDS and STRUCTURES
www.elsevier.com/locate/ijsolstr

Love waves in functionally graded piezoelectric materials

X.Y. Li *, Z.K. Wang *, S.H. Huang

Department of Engineering Mechanics, Xi'an Jiaotong University, Xi'an 710049, People's Republic of China

Received 26 May 2004
Available online 3 August 2004

Abstract

To investigate the features of Love waves in a layered functionally graded piezoelectric structure, the mathematical model is established on the basis of the elastic wave theory, and the WKB method is applied to solve the coupled electromechanical field differential equation. The solutions of the mechanical displacement and electrical potential function are obtained for the piezoelectric layer and elastic substrate. The dispersion relations of Love waves are deduced for electric open and short cases on the free surface respectively. The actual piezoelectric layer–elastic substrate systems are taken into account, and some corresponding numerical examples are proposed comparatively. Thus, the effects of the gradient variation about material constants on the phase velocity, the group velocity, the coupled electromechanical factor and the cutoff frequency are discussed in detail. So the propagation behaviors of Love waves in inhomogeneous medium is revealed, and the dispersion and the anti-dispersion are analyzed. The conclusions are significant both theoretically and practically for the surface acoustic wave devices.

Keywords: Love waves; Functionally graded piezoelectric materials; WKB method; Dispersion equation

1. Introduction

In recent years, a new-style material called functionally graded material (FGM) has come Out. Because of the superiority over many composite materials, FGMs have been used not only in the spaceflight and aerospace but also in electronic and electric fields. With the development of the material technology, the functionally graded piezoelectric material (FGPM) is manufactured. To improve the efficiency and natural life of the surface acoustic wave (SAW) devices, FGPM is considered to apply in SAW devices. Hence, the study of wave propagation behaviors and characteristics in FGPM has become a topic of practical importance.

Elastic wave propagation in layered piezoelectric media are given to considerable attention previously exhibited by the literature of Pauley and Dong (1976), Shiosai et al. (1986), Siao and Dong (1994) and Wang and Quek (2001). Furthermore, there have also been many works about wave characteristics and

* Corresponding authors. Tel.: +8601062778612; fax: +8601062781824.
E-mail addresses: lxy9977@ccermail.net (X.Y. Li), zkwang@mail.xjtu.edu.cn (Z.K. Wang).

0020-7683/$ - see front matter © 2004 Elsevier Ltd. All rights reserved.
doi:10.1016/j.ijsolstr.2004.05.064

transient response of FGM structures. Liu et al. (1991a) and Liu and Tani (1992) have investigated surface waves in FGM plates with the application of strip element method. Ohyoshi (1993, 1995) and Ohyoshi et al. (1996) proposed an analytical method to analyze wave reflection and transmission for an FGM plate. Liu et al. (1999) and Han et al. (2000) discussed stress waves in FGMs using linearly inhomogeneous elements (LIEs) and quadratic layer elements, respectively. Han et al. (2001, 2002) have introduced a hybrid numerical method (HNM) for analyzing characteristics of waves and transient responses in FGM cylinders.

Over the past decade, wave propagation problems related to FGPM have been widely studied. HNM which combines the finite element method with the Fourier transformation method, was proposed for characteristics and response of wave propagation in FGPM (Liu and Tani, 1991, 1994). Recently, Liu et al. (2003) provided piezoelectricity effects on the dispersion and characteristics of waves in FGPM plates through the introduction of LIEs. Using an analytical-numerical method, Han and Liu (2003) investigated the frequency and group velocity dispersion behaviors, and characteristic surfaces of waves in FGPM cylinders.

In this paper, the motion differential equations of the wave, considering that the material properties of the FGPM guiding layer change continuously in the thickness direction, are presented to obtain the dispersion of Love waves. The WKB method is used to solve the coupled electromechanical field differential equations. The dispersion relations for the electric open and short cases are formulated with the aid of the mechanical displacement and electrical potential function. The influences of the gradient of the material constants on the phase velocity, the group velocity, the coupled electromechanical factor and the cutoff frequency, are clarified by some numerical simulations. Finally, the qualitative properties of Love wave propagation in the inhomogeneous material are illustrated.

This paper presents a mathematics approximation method which has usually been called the WKB method. The method which was first proposed in the mid-1920s by Wentzel, Kramers, Brillouin and Jeffreys, has in reality been known for a long time. The method describes various kinds of wave motion in an inhomogeneous medium, where the properties change only slightly over one wavelength, and it also provides the connection between classical mechanics and quantum mechanics (Nanny and Per Olof, 2002). The traditional WKB method has served amazingly well in a variety of problems, especially in problems of quantum mechanics, nonuniform waveguides and atomic physics. Since the material constant of the FGPM is nonuniform, the WKB method springs for obtaining the solution of the governing differential equations of wave motion.

2. Statement of the problem

Consider a layered half-space of a semi-finite substrate covered with a FGPM medium on the surface, such as shown in Fig. 1. The piezoelectric layer with a thickness h is transversely isotropic, and the elastic substrate is isotropic. The rectangular Cartesian coordinates (x, y, z) are selected so that the z-axis consisted with the polarization direction of the piezoelectric layer and perpendicular to the x–y plane. It is assumed that the upper surface of the guiding layer is stress free, and the substrate is bonded ideally with the layer. Here, Love waves propagating along the y-axis are studied mainly.

For an FGPM medium, the constitutive equations are

$$\left.\begin{aligned} \sigma_{ij} &= c_{ijkl}S_{kl} - e_{kij}E_k \\ D_j &= e_{jkl}S_{kl} + \varepsilon_{jk}E_k \end{aligned}\right\}, \tag{1}$$

where σ_{ij}, S_{kl}, E_k and D_j indicate the stress tensor, strain tensor, electric field vector and electric displacement vector, respectively. c_{ijkl}, e_{kij} and ε_{jk}, which vary continuously in the thickness direction, are the elastic, piezoelectric and dielectric constants. The equations of motion are given by

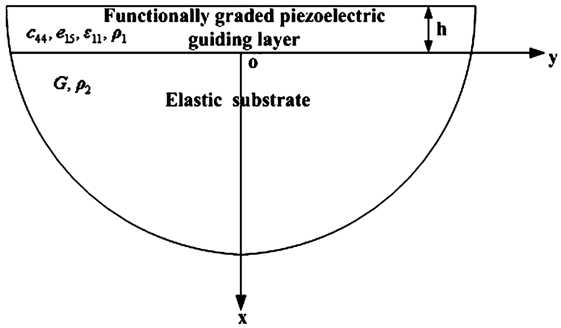

Fig. 1. Layered FGPM half-space.

$$\left.\begin{aligned}\sigma_{ij,j} &= \rho \ddot{u}_i \\ D_{i,i} &= 0\end{aligned}\right\}, \tag{2}$$

where "$\cdot$" denotes the differentiation with respect to time t , "," denotes the space-coordinate differentiation, while ρ is the density of the material, u the mechanical displacement.

The relationship between the displacement components and strain components is given by

$$S_{ij} = \frac{1}{2}(u_{i,j} + u_{j,i}). \tag{3a}$$

The Maxwell equations in the quasi-static approximation are

$$E_i = -\varphi_{,i}, \tag{3b}$$

where φ is the electrostatic potential. Eq. (3a) and Eq. (3b) are called geometrical equations.

For a transversely isotropic piezoelectric layer, Eq. (1) can be written as

$$\left.\begin{aligned}\sigma_x &= c_{11}S_x + c_{12}S_y + c_{13}S_z - e_{31}E_z \\ \sigma_y &= c_{12}S_x + c_{11}S_y + c_{13}S_z - e_{31}E_z \\ \sigma_z &= c_{13}S_x + c_{13}S_y + c_{33}S_z - e_{31}E_z \\ \tau_{yz} &= c_{44}S_{yz} - e_{15}E_y \\ \tau_{zx} &= c_{44}S_{zx} - e_{15}E_x \\ \tau_{xy} &= \frac{c_{11} - c_{12}}{2}S_{xy}\end{aligned}\right\}, \tag{4a}$$

$$\left.\begin{aligned}D_x &= e_{15}S_{zx} + \varepsilon_{11}E_x \\ D_y &= e_{15}S_{yz} + \varepsilon_{11}E_y \\ D_z &= e_{31}S_x + e_{31}S_y + e_{33}S_z + \varepsilon_{33}E_z\end{aligned}\right\}, \tag{4b}$$

in which the elastic constants c_{ij}, piezoelectric constants e_{ij} and dielectric constants ε_{ij} $(i, j = 1, 2, \ldots, 6)$ are function of x, i.e. $c_{ij} \equiv c_{ij}(x), e_{ij} \equiv e_{ij}(x), \varepsilon_{ij} \equiv \varepsilon_{ij}(x)$.

It is assumed that Love waves propagate in the positive direction of y-axis, we have

$$u = v = 0, \quad w = w(x, y, t), \quad \varphi = \varphi(x, y, t). \tag{5}$$

Let w_1 and φ_1 denote the mechanical displacement and electric potential function in the region $-h < x < 0$, then using Eqs. (2) and (5), as well as Eqs. (3) and (4), we obtain the following field equations for the piezoelectric layer:

$$\left.\begin{aligned}c_{44}\left(\frac{\partial^2 w_1}{\partial x^2}+\frac{\partial^2 w_1}{\partial y^2}\right)+e_{15}\left(\frac{\partial^2 \varphi_1}{\partial x^2}+\frac{\partial^2 \varphi_1}{\partial y^2}\right)+c'_{44}\frac{\partial w_1}{\partial x}+e'_{15}\frac{\partial \varphi_1}{\partial x}=\rho_1\frac{\partial^2 w_1}{\partial t^2}\\ e_{15}\left(\frac{\partial^2 w_1}{\partial x^2}+\frac{\partial^2 w_1}{\partial y^2}\right)-\varepsilon_{11}\left(\frac{\partial^2 \varphi_1}{\partial x^2}+\frac{\partial^2 \varphi_1}{\partial y^2}\right)+e'_{15}\frac{\partial w_1}{\partial x}-\varepsilon'_{11}\frac{\partial \varphi_1}{\partial x}=0\end{aligned}\right\}, \tag{6}$$

where "′" denote the differentiation with respect to x.

Let w_2 and φ_2 denote the mechanical displacement and electric potential function in the region $x>0$. According to the general elastic theory, the field equations for elastic substrate can be obtained as follows:

$$\left.\begin{aligned}G\left(\frac{\partial^2 w_2}{\partial x^2}+\frac{\partial^2 w_2}{\partial y^2}\right)=\rho_2\frac{\partial^2 w_2}{\partial t^2}\\ \frac{\partial^2 \varphi_2}{\partial x^2}+\frac{\partial^2 \varphi_2}{\partial y^2}=0\end{aligned}\right\}, \tag{7}$$

where G is the shear modulus. In general, the upper surface of the piezoelectric layer is in air, and the dielectric constant ε_0 of air is much smaller than that of the piezoelectric medium. So air can be treated as vacuum. Such that the electric potential function φ_0 for air ($x<-h$) satisfies Laplace's equation, i.e.

$$\frac{\partial^2 \varphi_0}{\partial x^2}+\frac{\partial^2 \varphi_0}{\partial y^2}=0. \tag{8}$$

Furthermore, we take into account the boundary and continuous conditions at the free surface and the interface of the layer-substrate system. And two kinds of electrical boundary conditions, i.e. electrical open and short conditions, would be considered at the top of the structure.

- At the free surface of the layer, i.e. $x=-h$

$$\left.\begin{aligned}\tau_{zx1}(-h,y)=0\\ \varphi_1(-h,y)=\varphi_0(-h,y)\\ D_{x1}(-h,y)=D_{x0}(-h,y)\end{aligned}\right\}\quad \text{(electric open case)}$$

or

$$\left.\begin{aligned}\tau_{zx1}(-h,y)=0\\ \varphi_1(-h,y)=0\end{aligned}\right\}\quad \text{(electric short case)}.$$

- At the interface of two materials, i.e. $x=0$

$$\left.\begin{aligned}w_1(0,y)=w_2(0,y)\\ \tau_{zx1}(0,y)=\tau_{zx2}(0,y)\\ \varphi_1(0,y)=\varphi_2(0,y)\\ D_{x1}(0,y)=D_{x2}(0,y)\end{aligned}\right\}.$$

- For $x\to+\infty$, $w_2\to 0$, $\varphi_2\to 0$. For $x\to-\infty$, $\varphi_0\to 0$.

3. Solutions of the problem

Assuming the solutions of Eq. (6) as follows:

$$\left.\begin{aligned}w_1(x,y,t)=W_1(x,y)e^{i(ky-k_0ct)}\\ \varphi_1(x,y,t)=\Phi_1(x,y)e^{i(ky-k_0ct)}\end{aligned}\right\}, \tag{9}$$

and substituting Eq. (9) into Eq. (6), we obtain

$$\left.\begin{array}{l} c_{44}\left(\dfrac{\partial^2 W_1}{\partial x^2}+\dfrac{\partial^2 W_1}{\partial y^2}\right)+c'_{44}\dfrac{\partial W_1}{\partial x}+2\mathrm{i}k_0c_{44}\dfrac{\partial W_1}{\partial y}+\left(\rho_1c^2-c_{44}\right)k_0^2W_1 \\ +e_{15}\left(\dfrac{\partial^2 \Phi_1}{\partial x^2}+\dfrac{\partial^2 \Phi_1}{\partial y^2}\right)+e'_{15}\dfrac{\partial \Phi_1}{\partial x}+2\mathrm{i}k_0e_{15}\dfrac{\partial \Phi_1}{\partial y}-k_0^2e_{15}\Phi_1=0 \\ e_{15}\left(\dfrac{\partial^2 W_1}{\partial x^2}+\dfrac{\partial^2 W_1}{\partial y^2}\right)+e'_{15}\dfrac{\partial W_1}{\partial x}+2\mathrm{i}k_0e_{15}\dfrac{\partial W_1}{\partial y}-k_0^2e_{15}W_1 \\ -\varepsilon_{11}\left(\dfrac{\partial^2 \Phi_1}{\partial x^2}+\dfrac{\partial^2 \Phi_1}{\partial y^2}\right)-\varepsilon'_{11}\dfrac{\partial \Phi_1}{\partial x}-2\mathrm{i}k_0\varepsilon_{11}\dfrac{\partial \Phi_1}{\partial y}+k_0^2\varepsilon_{11}\Phi_1=0 \end{array}\right\}, \tag{10}$$

where k_0 is the wave number for the homogeneous piezoelectric layer, and c is the phase velocity of wave propagation, while $W_1(x,y)$ and $\Phi_1(x,y)$ are the unknown functions given by

$$\left.\begin{array}{l} W_1(x,y)=X_1(x)Y_1(y) \\ \Phi_1(x,y)=\overline{X}_1(x)\overline{Y}_1(y) \end{array}\right\}, \tag{11}$$

in which $Y_1(y)\equiv\overline{Y}_1(y)\equiv Y(y)$. Substitution Eq. (11) into Eq. (10) leads to the following differential equations:

$$\left.\begin{array}{l} c_{44}(x)\left\{X_1''(x)+c'_{44}(x)X_1'(x)/c_{44}(x)+\left[\rho_1c^2k_0^2/c_{44}(x)-k^2\right]X_1(x)\right\} \\ \quad +e_{15}(x)\left[\overline{X}_1''(x)+e'_{15}(x)\overline{X}_1'(x)/e_{15}(x)-k^2\overline{X}_1(x)\right]=0 \\ e_{15}(x)\left[X_1''(x)+e'_{15}(x)\overline{X}_1'(x)/e_{15}(x)-k^2X_1(x)\right] \\ \quad -\varepsilon_{11}(x)\left[\overline{X}_1''(x)+\varepsilon'_{11}(x)\overline{X}_1'(x)/\varepsilon_{11}(x)-k^2\overline{X}_1(x)\right]=0 \end{array}\right\}, \tag{12}$$

$$Y''(y)+2\mathrm{i}k_0Y'(y)+(\Delta k^2)Y(y), \tag{13}$$

where $k^2=k_0^2+(\Delta k)^2$, $(\Delta k)^2$ remains constant.

Applying the separate variable method and noting the wave propagation direction, we can obtain the solutions of Eq. (7),

$$\left.\begin{array}{l} w_2(x,y,t)=A_2\mathrm{e}^{-kb_2x}\mathrm{e}^{\mathrm{i}(ky-k_0ct)} \\ \varphi_2(x,y,t)=B_2\mathrm{e}^{-kx}\mathrm{e}^{\mathrm{i}(ky-k_0ct)} \end{array}\right\}, \tag{14}$$

where $b_2=\sqrt{k^2-\rho_2c^2k_0^2/G}$.

With the help of the third boundary condition in Section 2, the solution of the electric potential function in vacuum is obtained from Eq. (8),

$$\varphi_0(x,y,t)=A_0\mathrm{e}^{kx}\mathrm{e}^{\mathrm{i}(ky-k_0ct)}. \tag{15}$$

3.1. Assumption

One of essential features about FGMs includes the tailoring of chemical composition and microstructure in an intentional artificial manner on basis of quantitative prediction of the profile of properties distribution to achieve the desired function (Kawasaki and Watanabe, 1997). In practice, the improvement of piezoelectricity is the key to fabrication of FGPMs. The powder metallurgical processing for fabricating FGPMs is quite complicated at present, and it is difficult to estimate material property changes synchronously in term of a certain law.

When investigating crack in FGPMs, Wang (2003) and Ueda (2003) assumed that the variations of the material properties are in the same proportion in order to overcome the complexity of mathematics involved. For simplicity, we consider that the variations in material constants are independent through the thickness. In Section 6, we can find that gradient variations of material constants have different effects on the dispersive characteristics of waves. Through this assumption, the effects of the different material constants on Love waves are decoupled.

3.2. Gradient variation in the piezoelectric constant

The material property vary according to the following law:

$$e_{15}(x) = e_{15}^0 \exp(\alpha x/h), \quad c_{44}(x) = c_{44}^0, \quad \varepsilon_{11}(x) = \varepsilon_{11}^0, \tag{16}$$

where e_{15}^0, c_{44}^0 and ε_{11}^0 are the piezoelectric, elastic and dielectric constants at $x = 0$, respectively; α is the gradient coefficient. Regarding α as a small parameter and substituting Eq. (16) into Eq. (12), we obtain

$$\left.\begin{array}{l} p_e(x)X_1''(x) + \left\{[\beta - p_e(x)]k^2 - \beta(\Delta k)^2\right\}X_1(x) = 0 \\ \overline{X}_1''(x) - k^2\overline{X}_1(x) = -\beta k_0^2 e_{15}(x)X_1(x)/\left[\varepsilon_{11}^0 p_e(x)\right] \end{array}\right\}, \tag{17}$$

where $p_e(x) = c_{44}^0\varepsilon_{11}^0 + e_{15}^2(x)$, $\beta = \varepsilon_{11}^0\rho_1 c^2$. Using the phase integral approach,

$$X_1(x) = \exp\left(\int \phi(x)\mathrm{d}x\right), \tag{18}$$

then substituting this into Eq. (17), we have

$$p_e(x)\left[\phi^2(x) + \phi'(x)\right] + \left\{[\beta - p_e(x)]k^2 - \beta(\Delta k)^2\right\} = 0. \tag{19}$$

Note that Eq. (19) is a first-order nonlinear differential equation. The asymptotically solution of ϕ is approximated as

$$\phi(x) = \phi_0(x)k + \phi_1(x) + \phi_2(x)/k + \cdots. \tag{20}$$

Substituting Eq. (20) into Eq. (19) and equating the coefficients of each power of k to zero, we get an infinite number of equations. The first three are

$$\begin{array}{l} p_e(x)\phi_0^2(x) + \beta - p_e(x) = 0, \\ 2p_e(x)\phi_0(x)\phi_1(x) + p_e(x)\phi_0'(x) = 0, \\ 2p_e(x)\phi_0(x)\phi_2(x) + p_e(x)\phi_1^2(x) + p_e(x)\phi_1'(x) - \beta(\Delta k)^2 = 0. \end{array}$$

Their solutions are obtained as follows:

$$\begin{array}{l} \phi_0^{(1)} = \mathrm{i}\sqrt{\beta/p_e(x) - 1}, \quad \phi_0^{(2)} = -\mathrm{i}\sqrt{\beta/p_e(x) - 1}, \\ \phi_1^{(1)} = \phi_1^{(2)} = 0, \\ \phi_2^{(1)} = -\dfrac{\mathrm{i}\beta(\Delta k)^2}{2\sqrt{[\beta - p_e(x)]p_e(x)}}, \quad \phi_2^{(2)} = \dfrac{i\beta(\Delta k)^2}{2\sqrt{[\beta - p_e(x)]p_e(x)}}. \end{array}$$

Recurring to the exponential transformation Eq. (18), we get

$$X_1(x) = C_1\mathrm{e}^{\mathrm{i}kb_1q_e(x)} + C_2\mathrm{e}^{-\mathrm{i}kb_1q_e(x)},$$

where C_1 and C_2 are unknown constants. Furthermore, the parameter b_1 and the function $q_e(x)$ are given as

$$b_1 = \sqrt{\beta/p_e(0) - 1} = \sqrt{\frac{\varepsilon_{11}^0 \rho_1 c^2}{c_{44}^0 \varepsilon_{11}^0 + (e_{15}^0)^2} - 1},$$

$$q_e(x) = \frac{h}{2\alpha b_1}\left\{ \arctan\left[\frac{\beta - 2p_e(x)}{2\sqrt{[\beta - p_e(x)]p_e(x)}}\right] + \left[\frac{\beta}{2\sqrt{(\beta-\gamma)\gamma}} \cdot \frac{k^2 - k_0^2}{k^2} - \sqrt{\frac{\beta-\gamma}{\gamma}}\right]\left[\ln\left[2\gamma(\beta - p_e(x)) + \beta e_{15}^2(x) + 2\sqrt{\gamma p_e(x)(\beta-\gamma)[\beta - p_e(x)]}\right] - \frac{2\alpha x}{h}\right]\right\},$$

where $\gamma = c_{44}^0 \varepsilon_{11}^0$. The foregoing asymptotic expansion approximation is named WKB method (Ghatak et al., 1991).

The special solution to the second equation of Eq. (12) is

$$\overline{X}_1(x) = f(x)X_1(x) = f(x)\exp\left(\int \phi(x)\mathrm{d}x\right).$$

Substituting this into Eq. (12), applying the WKB method and combining with the general solution we obtain

$$\overline{X}_1(x) = C_3 e^{kx} + C_4 e^{-kx} + \frac{e_{15}(x)}{\varepsilon_{11}^0}\left[C_1 e^{ikb_1 q_e(x)} + C_2 e^{-ikb_1 q_e(x)}\right].$$

And Eq. (13) gives the following solution:

$$Y(x) = C e^{i(k-k_0)y}.$$

Therefore, the solution of the mechanical displacement and electric potential function for the guiding layer in the case of the piezoelectric constant variation is

$$\left.\begin{aligned} w_1(x,y,t) &= \left[A_1 e^{ikb_1 q_e(x)} + B_1 e^{-ikb_1 q_e(x)}\right] e^{i(ky - k_0 ct)} \\ \varphi_1(x,y,t) &= \left\{\frac{e_{15}(x)}{\varepsilon_{11}^0}\left[A_1 e^{ikb_1 q_e(x)} + B_1 e^{-ikb_1 q_e(x)}\right] + D_1 e^{kx} + M_1 e^{-kx}\right\} e^{i(ky - k_0 ct)} \end{aligned}\right\}. \tag{21}$$

3.3. Gradient variation in the dielectric constant

It is assumed that the dielectric constant changes continuously in the thickness direction and the material property variation conform to the following exponential law:

$$\varepsilon_{11}(x) = \varepsilon_{11}^0 \exp(\eta x/h), \quad e_{15}(x) = e_{15}^0, \quad c_{44}(x) = c_{44}^0,$$

where η is the gradient coefficient. In the same manner, we can obtain the solution of the mechanical displacement and electric potential function for the layer in the case of the dielectric constant variation as follows:

$$\left.\begin{aligned} w_1(x,y,t) &= \left[A_1 e^{ikb_1 q_\varepsilon(x)} + B_1 e^{-ikb_1 q_\varepsilon(x)}\right] e^{i(ky - k_0 ct)} \\ \varphi_1(x,y,t) &= \left\{\frac{e_{15}^0}{\varepsilon_{11}(x)}\left[A_1 e^{ikb_1 q_\varepsilon(x)} + B_1 e^{-ikb_1 q_\varepsilon(x)}\right] + D_1 e^{kx} + M_1 e^{-kx}\right\} e^{i(ky - k_0 ct)} \end{aligned}\right\}. \tag{22}$$

where the function $q_\varepsilon(x)$ is obtained in the following form:

$$q_\varepsilon(x) = -\frac{h}{\eta b_1}\left\{ \arctan\left[\frac{\beta - 2\bar{p}_\varepsilon(x)}{2\sqrt{\left[\beta - \bar{p}_\varepsilon(x)\right]\bar{p}_\varepsilon(x)}}\right] + \left[\frac{\beta}{2\sqrt{(\beta-\gamma)\gamma}}\cdot\frac{k^2-k_0^2}{k^2} - \sqrt{\frac{\beta-\gamma}{\gamma}}\right] \times \left[\ln\left[2\gamma\left(\beta - \bar{p}_\varepsilon(x)\right) + \beta\left(e_{15}^0\right)^2 e^{-\eta x/h} + 2\sqrt{\gamma\bar{p}_\varepsilon(x)(\beta-\gamma)\left[\beta - \bar{p}_\varepsilon(x)\right]}\right] + \frac{\eta x}{h}\right]\right\}$$

with $\bar{p}_\varepsilon(x) = \gamma + \left(e_{15}^0\right)^2 e^{-\eta x/h}$.

3.4. Gradient variation in the elastic constant

The material properties of the layer vary as the following function:

$$c_{44}(x) = c_{44}^0 \exp(\xi x/h), \quad e_{15}(x) = e_{15}^0, \quad \varepsilon_{11}(x) = \varepsilon_{11}^0,$$

where ξ is the gradient coefficient. The WKB method is still applied to solve the differential equation, but the gradient coefficient ξ is unnecessary to consider a small parameter. Finally the solution in the case of the elastic constant variation is

$$\left.\begin{aligned} w_1(x,y,t) &= \left[A_1 e^{ikb_1 q_c(x)} + B_1 e^{-ikb_1 q_c(x)}\right] e^{kg(x)} e^{i(ky-k_0ct)} \\ \varphi_1(x,y,t) &= \left\{\frac{e_{15}^0}{\varepsilon_{11}^0}\left[A_1 e^{ikb_1 q_c(x)} + B_1 e^{-ikb_1 q_c(x)}\right] e^{kg(x)} + D_1 e^{kx} + M_1 e^{-kx}\right\} e^{i(ky-k_0ct)} \end{aligned}\right\} \tag{23}$$

in which the functions $g(x)$ and $q_c(x)$ are express as

$$g(x) = -\frac{1}{4k}\ln\{[\beta - p_c(x)]p_c(x)\},$$

$$q_c(x) = \frac{h}{\xi b_1}\left\{ \arctan\left[\frac{\beta - 2p_c(x)}{2\sqrt{[\beta - p_c(x)]p_c(x)}}\right] - \left[-\sqrt{\frac{\beta - \left(e_{15}^0\right)^2}{\left(e_{15}^0\right)^2}}\right]\left[\ln\left[2\left(e_{15}^0\right)^2[\beta - p_c(x)] + \beta\varepsilon_{11}^0 c_{44}(x) + 2\sqrt{\left(e_{15}^0\right)^2\left[\beta - \left(e_{15}^0\right)^2\right]p_c(x)[\beta - p_c(x)]}\right] - \frac{\xi x}{h}\right]\right\}$$

with $p_c(x) = c_{44}(x)\varepsilon_{11}^0 + \left(e_{15}^0\right)^2$.

4. Dispersion equation

4.1. Gradient variation in the piezoelectric constant

For the case of the electric open, substituting Eqs. (14), (15), (21) and their corresponding stress and electric displacement components into the boundary and continuous conditions, we obtain the following the algebraic equations about the unknown constants A_1, B_1, D_1, M_1, A_2, B_2 and A_0:

$$\left.\begin{array}{l}
\dfrac{\mathrm{i}b_1p_e(-h)q_e'(-h)}{\varepsilon_{11}^0}\left[A_1\mathrm{e}^{\mathrm{i}kb_1q_e(-h)}-B_1\mathrm{e}^{-\mathrm{i}kb_1q_e(-h)}\right]+e_{15}(-h)\left(D_1\mathrm{e}^{-kh}-M_1\mathrm{e}^{kh}\right)=0\\
\dfrac{e_{15}(-h)}{\varepsilon_{11}^0}\left[A_1\mathrm{e}^{\mathrm{i}kb_1q_e(-h)}+B_1\mathrm{e}^{-\mathrm{i}kb_1q_e(-h)}\right]+D_1\mathrm{e}^{-kh}+M_1\mathrm{e}^{kh}-A_0\mathrm{e}^{-kh}=0\\
\varepsilon_{11}^0(-D_1\mathrm{e}^{-kh}+M_1\mathrm{e}^{kh})+A_0\varepsilon_0\mathrm{e}^{-kh}=0\\
\dfrac{\mathrm{i}b_1p_e(0)q_e'(0)}{\varepsilon_{11}^0}\left[A_1\mathrm{e}^{\mathrm{i}kb_1q_e(0)}-B_1\mathrm{e}^{-\mathrm{i}kb_1q_e(0)}\right]+e_{15}^0(D_1-M_1)+A_2Gb_2=0\\
A_1\mathrm{e}^{\mathrm{i}kb_1q_e(0)}+B_1\mathrm{e}^{-\mathrm{i}kb_1q_e(0)}-A_2=0\\
\dfrac{e_{15}^0}{\varepsilon_{11}^0}\left[A_1\mathrm{e}^{\mathrm{i}kb_1q_e(0)}+B_1\mathrm{e}^{-\mathrm{i}kb_1q_e(0)}\right]+D_1+M_1-B_2=0\\
\varepsilon_0(-D_1+M_1)-B_2\varepsilon_2=0
\end{array}\right\}, \tag{24}$$

where ε_2 is the dielectric constant of the substrate, and the function $q_e'(x)$ is

$$q_e'(x)=\frac{1}{b_1}\left\{\sqrt{\frac{\beta}{p_e(x)}-1}-\frac{\beta}{2\sqrt{[\beta-p_e(x)]p_e(x)}}\cdot\frac{k^2-k_0^2}{k^2}\right\}.$$

If there exit nontrivial solutions of Eq. (24), the determinant of the coefficient matrix of Eq. (24) must equal to zero, i.e.

$$\begin{aligned}
&V_{eh}e_{15}^h[\chi_2\sinh(kh)+\cosh(kh)][-Gb_2\sin(kb_1q_{eh0})+T_{e0}\cos(kb_1q_{eh0})]-T_{eh}[(\chi_0\chi_2+1)\sinh(kh)\\
&\quad+(\chi_0+\chi_2)\cosh(kh)][T_{e0}\sin(kb_1q_{eh0})+Gb_2\cos(kb_1q_{eh0})]+V_0T_{eh}e_{15}^0[\chi_0\sinh(kh)\\
&\quad+\cosh(kh)]\cos(kb_1q_{eh0})+V_{eh}V_0e_{15}^he_{15}^0\sinh(kh)\sin(kb_1q_{eh0})-\left(T_{eh}V_{eh}e_{15}^0+T_{e0}V_0e_{15}^h\right)\\
&\quad=0,
\end{aligned}\tag{25}$$

where

$$\begin{aligned}
&V_{eh}=e_{15}^h/\varepsilon_{11}^0,\quad V_0=e_{15}^0/\varepsilon_{11}^0,\quad \chi_0=\varepsilon_{11}^0/\varepsilon_0,\quad \chi_2=\varepsilon_{11}^0/\varepsilon_2,\quad e_{15}^h=e_{15}(-h),\\
&T_{eh}=b_1p_e(-h)q_e'(-h)/\varepsilon_{11}^0,\quad T_{e0}=b_1p_e(0)q_e'(0)/\varepsilon_{11}^0,\quad q_{eh0}=q_{eh}-q_{e0},\quad q_{eh}=q_e(-h),\quad q_{e0}=q_e(0).
\end{aligned}$$

In the same way we can obtain the following phase velocity equation for the electric short case

$$\begin{aligned}
&V_{eh}e_{15}^h[\chi_2\sinh(kh)+\cosh(kh)][-Gb_2\sin(kb_1q_{eh0})+T_{e0}\cos(kb_1q_{eh0})]-T_{eh}[\sinh(kh)+\chi_2\cosh(kh)]\\
&\quad\times[T_{e0}\sin(kb_1q_{eh0})+Gb_2\cos(kb_1q_{eh0})]+V_0T_{eh}e_{15}^0\cosh(kh)\cos(kb_1q_{eh0})+V_{eh}V_0e_{15}^he_{15}^0\sinh(kh)\\
&\quad\times\sin(kb_1q_{eh0})-(T_{eh}V_{eh}e_{15}^0+T_{e0}V_0e_{15}^h)\\
&\quad=0.
\end{aligned}\tag{26}$$

Eqs. (25) and (26) are called the dispersion equations of Love waves in the layered functionally graded piezoelectric structure for the electric open and short cases, respectively. Moreover, we can readily see that the phase velocity c is connected with the wave number (k and k_0), gradient, layer thickness and material constants.

4.2. Gradient variation in the dielectric constant

The same approach is introduced like the gradient variation of the piezoelectric constant, and the dispersion equations with the dielectric constant variation are expressed by

$$V_{\varepsilon h}e_{15}^{0}[\chi_2\sinh(kh)+\cosh(kh)][-Gb_2\sin(kb_1q_{\varepsilon h0})+T_{\varepsilon 0}\cos(kb_1q_{\varepsilon h0})]-T_{\varepsilon h}[(\chi_h\chi_2+1)\sinh(kh)+(\chi_h+\chi_2)\cosh(kh)][T_{\varepsilon 0}\sin(kb_1q_{\varepsilon h0})+Gb_2\cos(kb_1q_{\varepsilon h0})]+V_0T_{\varepsilon h}e_{15}^{0}[\chi_h\sinh(kh)+\cosh(kh)]\times\cos(kb_1q_{\varepsilon h0})+V_{\varepsilon h}V_0(e_{15}^{0})^2\sinh(kh)\sin(kb_1q_{\varepsilon h0})-(T_{\varepsilon h}V_{\varepsilon h}+T_{\varepsilon 0}V_0)e_{15}^{0}=0 \tag{27}$$

and

$$V_{\varepsilon h}e_{15}^{0}[\chi_2\sinh(kh)+\cosh(kh)][-Gb_2\sin(kb_1q_{\varepsilon h0})+T_{\varepsilon 0}\cos(kb_1q_{\varepsilon h0})]-T_{\varepsilon h}[\sinh(kh)+\chi_2\cosh(kh)]\times[T_{\varepsilon 0}\sin(kb_1q_{\varepsilon h0})+Gb_2\cos(kb_1q_{\varepsilon h0})]+V_0T_{\varepsilon h}e_{15}^{0}\cosh(kh)\cos(kb_1q_{\varepsilon h0})+V_{\varepsilon h}V_0(e_{15}^{0})^2\sinh(kh)\times\sin(kb_1q_{\varepsilon h0})-(T_{\varepsilon h}V_{\varepsilon h}+T_{\varepsilon 0}V_0)e_{15}^{0}=0, \tag{28}$$

where

$$V_{\varepsilon h}=e_{15}^{0}/\varepsilon_{11}^{h},\quad \chi_h=\varepsilon_{11}^{h}/\varepsilon_2,\quad \varepsilon_{11}^{h}=\varepsilon_{11}(-h),\quad q_{\varepsilon h0}=q_{\varepsilon h}-q_{\varepsilon 0}=q_\varepsilon(-h)-q_\varepsilon(0),$$

$$T_{\varepsilon h}=b_1p_\varepsilon(-h)q_\varepsilon'(-h)/\varepsilon_{11}^{h},\quad T_{\varepsilon 0}=b_1p_\varepsilon(0)q_\varepsilon'(0)/\varepsilon_{11}^{0},\quad p_\varepsilon(x)=c_{44}^{0}\varepsilon_{11}(x)+(e_{15}^{0})^2,$$

$$q_\varepsilon'(x)=\frac{1}{b_1}\left\{\sqrt{\frac{\beta}{\bar p_\varepsilon(x)}-1}-\frac{\beta}{2\sqrt{[\beta-\bar p_\varepsilon(x)]\bar p_\varepsilon(x)}}\cdot\frac{k^2-k_0^2}{k^2}\right\}.$$

Eqs. (27) and (28) are corresponding to the electric open and short, respectively.

4.3. Gradient variation in the elastic constant

According to the above approach, we also can obtain the dispersion equations as follows:

$$[(\chi_0+1)(\chi_2+1)H(kl_2)-(\chi_0-1)(\chi_2-1)H(kl_1)][(-T_{ch}T_{c0}-U_{ch}U_{c0}-U_{ch}Gb_2)\sin(kb_1q_{ch0})+(U_{ch}T_{c0}-T_{ch}U_{c0}-T_{ch}Gb_2)\cos(kb_1q_{ch0}]+V_0e_{15}^{0}[(\chi_0+1)H(kl_2)-(\chi_0-1)H(kl_1)][T_{ch}\times\cos(kb_1q_{ch0})+U_{ch}\sin(kb_1q_{ch0})]+V_0e_{15}^{0}[(\chi_2+1)H(kl_2)-(\chi_2-1)H(kl_1)][(-U_{c0}-Gb_2)\times\sin(kb_1q_{ch0})+T_{c0}\cos(kb_1q_{ch0})]+V_0^2(e_{15}^{0})^2[H(kl_2)-H(kl_1)]\sin(kb_1q_{ch0})-2T_{ch}V_0e_{15}^{0}H(2kg_h)-2T_{c0}V_0e_{15}^{0}H(2kg_0)=0 \tag{29}$$

and

$$[(\chi_2+1)H(kl_2)-(\chi_2-1)H(kl_1)][(-T_{ch}T_{c0}-U_{ch}U_{c0}-U_{ch}Gb_2)\sin(kb_1q_{ch0})+(U_{ch}T_{c0}-T_{ch}U_{c0}-T_{ch}Gb_2)\cos(kb_1q_{ch0})]+V_0e_{15}^{0}[H(kl_2)-H(kl_1)][T_{ch}\cos(kb_1q_{ch0})+U_{ch}\sin(kb_1q_{ch0})]+V_0e_{15}^{0}[(\chi_2+1)H(kl_2)-(\chi_2-1)H(kl_1)][(-U_{c0}-Gb_2)\sin(kb_1q_{ch0})+T_{c0}\cos(kb_1q_{ch0})]+V_0^2(e_{15}^{0})^2[H(kl_2)-H(kl_1)]\sin(kb_1q_{ch0})-2T_{ch}V_0e_{15}^{0}H(2kg_h)-2T_{c0}V_0e_{15}^{0}H(2kg_0)=0, \tag{30}$$

where

$$T_{ch} = b_1 p_c(-h) q_c'(-h)/\varepsilon_{11}^0, \quad T_{c0} = b_1 p_c(0) q_c'(0)/\varepsilon_{11}^0, \quad q_{ch0} = q_{ch} - q_{ch},$$

$$q_{ch} = q_c(-h), \quad q_{c0} = q_c(0), \quad l_1 = -h + g_h + g_0, \quad l_2 = h + g_h + g_0,$$

$$g_h = g(-h), \quad g_0 = g(0), \quad U_{ch} = p_c(-h) g'(-h)/\varepsilon_{11}^0, \quad U_{c0} = p_c(0) g'(0)/\varepsilon_{11}^0,$$

$$H(x) = \sinh(x) + \cosh(x).$$

Eq. (29) is for the electric open case, and Eq. (30) is for the electric short case.

4.4. Homogeneous piezoelectric layer

Note that $\alpha = 0$ corresponds to a homogeneous layer without change in the piezoelectric constant, under the consideration of $q_e(x) = x$, $k = k_0$, hence Eq. (25) and Eq. (26) are degenerated into the dispersion equations in a homogeneous piezoelectric layer for the electric open and short cases, respectively

$$\begin{aligned}&\vartheta[\chi_2 \sinh(k_0 h) + \cosh(k_0 h)]\{G b_2 \sin(k_0 h b_1)/[(c_{44} + \vartheta) b_1] + \cos(k_0 h b_1)\} + [(\chi_0 \chi_2 + 1) \sinh(k_0 h) \\ &\quad + (\chi_0 + \chi_2) \cosh(k_0 h)][(c_{44} + \vartheta) b_1 \sin(k_0 h b_1) - G b_2 \cos(k_0 h b_1)] + \vartheta[\chi_0 \sinh(k_0 h) + \cosh(k_0 h)] \\ &\quad \times \cos(k_0 h b_1) - \vartheta^2 \sinh(k_0 h) \sin(k_0 h b_1)/[(c_{44} + \vartheta) b_1] - 2\vartheta \\ &\quad = 0\end{aligned} \tag{31}$$

and

$$\begin{aligned}&\vartheta[\chi_2 \sinh(k_0 h) + \cosh(k_0 h)]\{G b_2 \sin(k_0 h b_1)/[(c_{44} + \vartheta) b_1] + \cos(k_0 h b_1)\} + [\sinh(k_0 h) + \chi_2 \\ &\quad \times \cosh(k_0 h)][(c_{44} + \vartheta) b_1 \sin(k_0 h b_1) - G b_2 \cos(k_0 h b_1)] + \vartheta \cosh(k_0 h) \cos(k_0 h b_1) - \vartheta^2 \sinh(k_0 h) \\ &\quad \times \sin(k_0 h b_1)/[(c_{44} + \vartheta) b_1] - 2\vartheta \\ &\quad = 0,\end{aligned} \tag{32}$$

where $\vartheta = (e_{15}^0)^2/\varepsilon_{11}^0$. The dispersion Eqs. (31) and (32) is the same as results obtained by Liu et al. (2001).

In case of $q_\varepsilon(x) = x$ and $k = k_0$, Eqs. (27) and (28) are changed into Eqs. (31) and (32). Similarly, Eqs. (29) and (30) are simplified to Eqs. (31) and (32) in case of $q_c(x) = x$, $g(x) = 0$ and $k = k_0$.

5. Mechanical displacements

For the electric open case, we can obtain from Eq. (24) that

$$B_1 = \zeta_e A_1, \tag{33}$$

where

$$\zeta_e = -\frac{\left[\varepsilon_2 V_0 + \frac{\varepsilon_2 - \varepsilon_{11}^0}{e_{15}^0}(\mathrm{i} T_{e0} + G b_2)\right] \mathrm{e}^{\mathrm{i} k b_1 q_{e0}} - \frac{\varepsilon_2}{\varepsilon_0}\left(\varepsilon_0 V_{eh} + \frac{\varepsilon_0 + \varepsilon_{11}^0}{e_{15}^h} \mathrm{i} T_{eh}\right) \mathrm{e}^{\mathrm{i} k b_1 q_{eh} + kh}}{\left[\varepsilon_2 V_0 + \frac{\varepsilon_2 - \varepsilon_{11}^0}{e_{15}^0}(-\mathrm{i} T_{e0} + G b_2)\right] \mathrm{e}^{-\mathrm{i} k b_1 q_{e0}} - \frac{\varepsilon_2}{\varepsilon_0}\left(\varepsilon_0 V_{eh} - \frac{\varepsilon_0 + \varepsilon_{11}^0}{e_{15}^h} i T_{eh}\right) \mathrm{e}^{-\mathrm{i} k b_1 q_{eh} + kh}}.$$

According to Eq. (33), the mechanical displacement can be rewritten by

$$w_1(x, y, t) = A_1\left[\mathrm{e}^{\mathrm{i} k b_1 q_e(x)} + \zeta_e \mathrm{e}^{-\mathrm{i} k b_1 q_e(x)}\right] \mathrm{e}^{\mathrm{i}(ky - k_0 ct)}.$$

When the dielectric and elastic constants vary continuously as the exponential law, the corresponding displacements in the layer for the electric open case can be obtained

$$w_1(x,y,t) = A_1\left[\mathrm{e}^{\mathrm{i}kb_1q_\varepsilon(x)} + \zeta_\varepsilon \mathrm{e}^{-\mathrm{i}kb_1q_\varepsilon(x)}\right]\mathrm{e}^{\mathrm{i}(ky-k_0ct)}$$

and

$$w_1(x,y,t) = A_1\left[\mathrm{e}^{\mathrm{i}kb_1q_c(x)} + \zeta_c \mathrm{e}^{-\mathrm{i}kb_1q_c(x)}\right]\mathrm{e}^{kg(x)}\mathrm{e}^{\mathrm{i}(ky-k_0ct)},$$

where

$$\zeta_\varepsilon = -\frac{\left[\varepsilon_2V_0 + \frac{\varepsilon_2-\varepsilon_{11}^0}{e_{15}^0}(\mathrm{i}T_{\varepsilon0}+Gb_2)\right]\mathrm{e}^{\mathrm{i}kb_1q_{\varepsilon0}} - \frac{\varepsilon_2}{\varepsilon_0}\left(\varepsilon_0V_{\varepsilon h} + \frac{\varepsilon_0+\varepsilon_{11}^h}{e_{15}^0}\mathrm{i}T_{\varepsilon h}\right)\mathrm{e}^{\mathrm{i}kb_1q_{\varepsilon h}+kh}}{\left[\varepsilon_2V_0 + \frac{\varepsilon_2-\varepsilon_{11}^0}{e_{15}^0}(-\mathrm{i}T_{\varepsilon0}+Gb_2)\right]\mathrm{e}^{-\mathrm{i}kb_1q_{\varepsilon0}} - \frac{\varepsilon_2}{\varepsilon_0}\left(\varepsilon_0V_{\varepsilon h} - \frac{\varepsilon_0+\varepsilon_{11}^h}{e_{15}^0}\mathrm{i}T_{\varepsilon h}\right)\mathrm{e}^{-ikb_1q_{\varepsilon h}+kh}},$$

$$\zeta_c = -\frac{\left[\varepsilon_2V_0 + \frac{\varepsilon_2-\varepsilon_{11}^0}{e_{15}^0}(\mathrm{i}T_{c0}+U_{c0}+Gb_2)\right]\mathrm{e}^{\mathrm{i}kb_1q_{c0}+kg_0} - \frac{\varepsilon_2}{\varepsilon_0}\left(\varepsilon_0V_0 + \frac{\varepsilon_0+\varepsilon_{11}^0}{e_{15}^0}(\mathrm{i}T_{ch}+U_{ch})\right)\mathrm{e}^{\mathrm{i}kb_1q_{ch}+kg_h+kh}}{\left[\varepsilon_2V_0 + \frac{\varepsilon_2-\varepsilon_{11}^0}{e_{15}^0}(-\mathrm{i}T_{c0}+U_{c0}+Gb_2)\right]\mathrm{e}^{-\mathrm{i}kb_1q_{c0}+kg_0} - \frac{\varepsilon_2}{\varepsilon_0}\left(\varepsilon_0V_0 + \frac{\varepsilon_0+\varepsilon_{11}^0}{e_{15}^0}(-\mathrm{i}T_{ch}+U_{ch})\right)\mathrm{e}^{-\mathrm{i}kb_1q_{ch}+kg_h+kh}}.$$

6. Numerical examples

In order to demonstrate the influences of the gradient on the phase velocity, the group velocity, the coupled electromechanical factor and the cutoff frequency, some simulations are proposed. And some interesting phenomena are mentioned in the discussion of the numerical results. As a sample, the set of FGPM layer-elastic substrate system is assumed, i.e. PZT-5H ceramic layer-SiO_2 glass substrate. The material constants for the piezoelectric layer and the elastic substrate are listed in Tables 1 and 2 (Liu et al., 2001), respectively. In addition, the other data are also given by, $h = 0.003$ m, $\varepsilon_0 = 8.85\times10^{-12}$ F/m.

And the following dimensionless parameters are introduced

$$\delta = \sqrt{|k^2-k_0^2|/k_0^2},\quad \omega = khc/c_{s1},\quad c_{sub} = c_{s2}/c_{s1},$$

where k and k_0 are the wave number in the FGPM and homogeneous layers, respectively; while c_{s1}, c_{s2} are the bulk shear velocity in the homogeneous piezoelectric layer and substrate, they are given by

$$c_{s1} = \sqrt{\frac{c_{44}^0\varepsilon_{11}^0 + (e_{15}^0)^2}{\varepsilon_{11}^0\rho_1}},\quad c_{s2} = \sqrt{\frac{G}{\rho_2}}.$$

Table 1
Material constants of the piezoelectric layer

Guiding layer	e_{15}^0 (c/m^2)	ε_{11}^0 (10^{-10} F/m)	c_{44}^0 (10^{10} N/m^2)	ρ_1 (10^3 kg/m^3)
PZT-5H ceramic	17.0	277.0	2.30	7.50

Table 2
Material constants of the elastic substrate

Elastic substrate	G (10^{10} N/m^2)	ε_2 (10^{-10} F/m)	ρ_2 (10^3 kg/m^3)
SiO_2 glass	3.12	0.366	2.20

6.1. Effect of gradient variation on the dispersive curves

Based on Eqs. (25)–(32), the dispersive curves for the electric open and short cases are plotted in Fig. 2. By comparison of the dispersion relation between the FGPM and homogeneous layer in Fig. 2, it is shown that the dispersive curves in the homogeneous system resemble those of the functionally gradient structure. From Fig. 2a and b, it can be seen that the phase velocity starts with c_{s2} and as the wave number increases, the phase velocity for the fundamental mode decreases and tends to c_{s1} at high wave numbers for the FGPM and homogeneous material. For a definite wave number, the phase velocity of FGPM is slightly larger than one of homogeneous material in Fig. 2a, whereas the opposite result is obtained in Fig. 2b. It is observed from Fig. 2c that the dispersive curves of FGPM are not monotonous any longer, when the gradient coefficient about the elastic constant is smaller. This can be explained through Fig. 6 in detail. However, the dispersive curves of FGPM will be monotonous in the case of larger elastic gradient, which are shown in Fig. 2d. Moreover, the initial phase velocity of FGPM is smaller than one of homogeneous material in Fig. 2c and d, especially for the fundamental mode. This is due to the fact that the elasticity effect on Love wave become stronger than the piezoelectricity effect, when the elastic constant of the piezoelectric layer vary in comparison with the substrate.

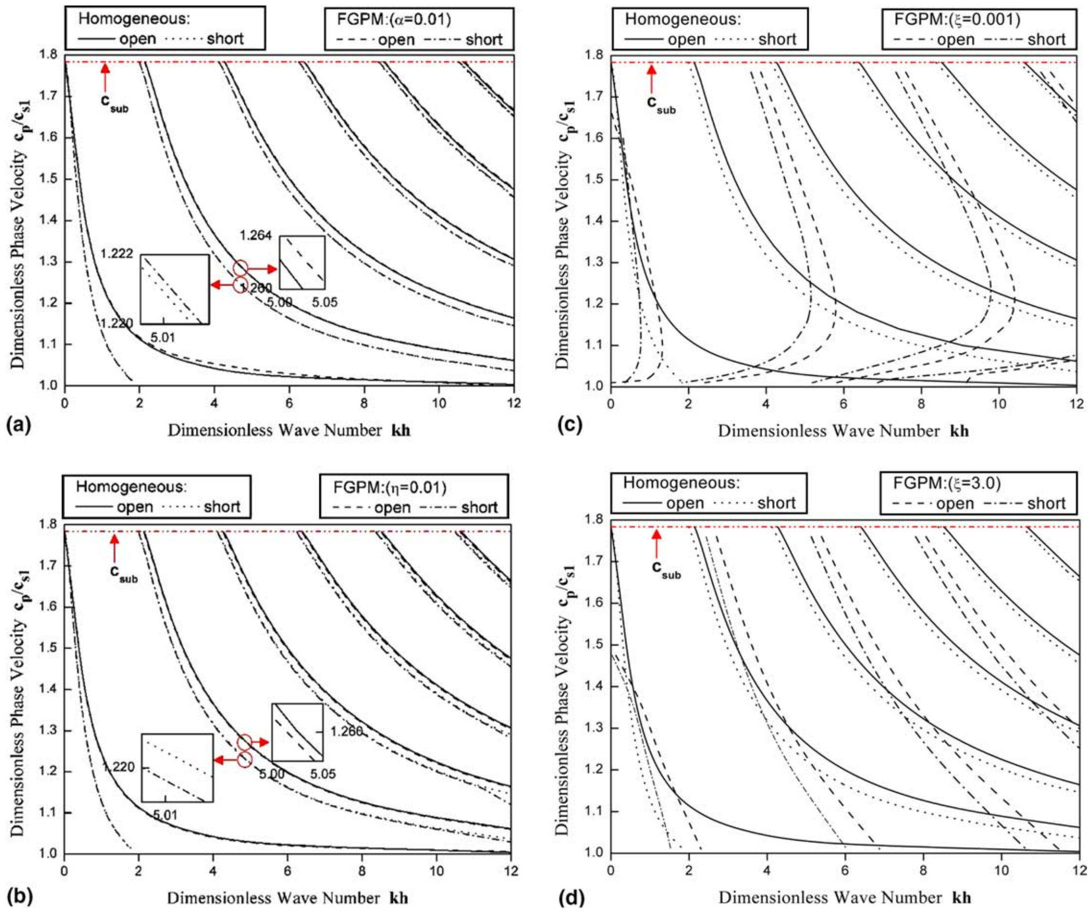

Fig. 2. Dispersive curves of Love waves in FGPM and homogeneous material.

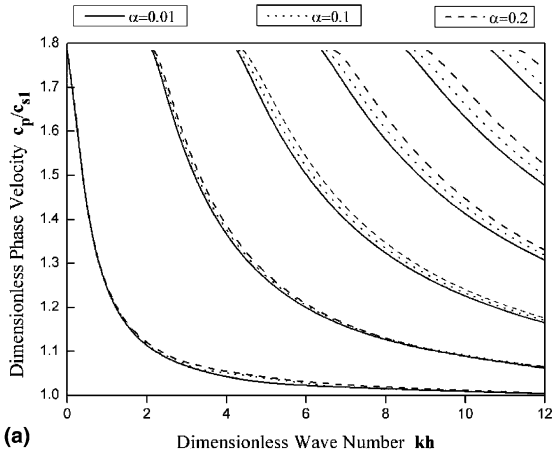

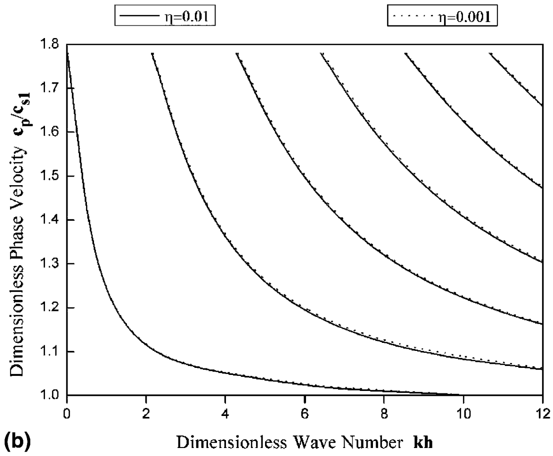

Fig. 3. Dispersive curses of Love waves in FGPM with the different gradient.

Variations of the dispersive curves for different gradients is shown in Fig. 3. From Fig. 3a, it can be remarked that the dispersive curves move right and the distance between the dispersion curves of each mode increase with the order of mode increasing, when the piezoelectric constant gradient become larger. That is to say, the phase velocity of Love waves increases with an increase of the gradient for the certain wave number or wavelength. The adverse results are remarked in Fig. 3b. This indicates that the efficiency of SAW devices with use of FGPM can be improved by adjusting the gradient of the piezoelectric and dielectric constants.

The relations between the modificatory coefficient δ and dimensionless frequency ω for the piezoelectric and dielectric constants variation, are shown as Fig. 4. In Fig. 4a, it can be seen that the gradient has a strong influence on the lower frequency for the fundamental mode, but the curves flat out after a sharp variation in a small lower frequency domain and tend to the unchangeable values in all three modes. The similar results as Fig. 4a can be observed in Fig. 4b. At higher frequency range, the wave number of Love waves in FGPM is 5%–5.8% greater than one in homogeneous material, while the gradient $\alpha = 0.01$. In practice, the piezoelectric effects become significant for large wave number (Liu et al., 2003). Therefore, if FGPM is applied to SAW devices, the piezoelectric effects will be prominent.

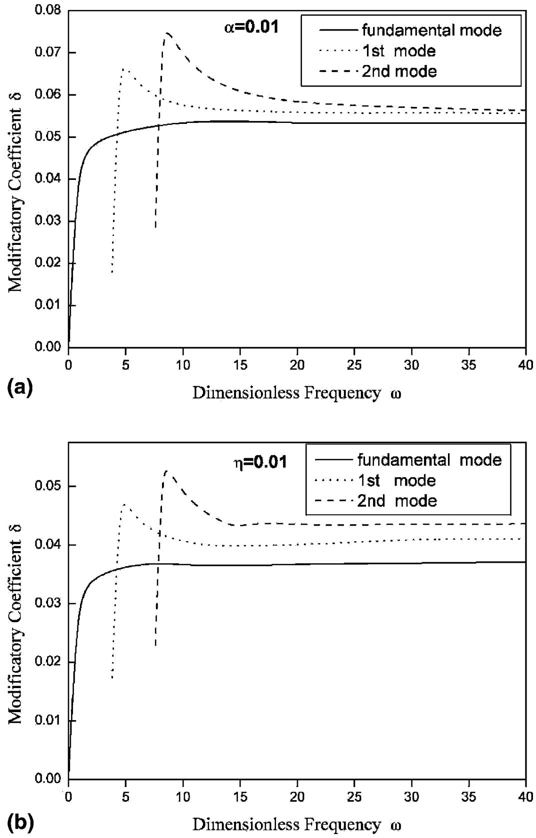

Fig. 4. Variation of the modificatory coefficient and dimensionless frequency.

To explain intensively the dispersion relation, the group velocity c_g is presented. It is well known that the group velocity expresses the rate at which energy is transported. The group velocity is defined as (Karl, 1975 and Julius, 1978)

$$c_g = c + k\frac{dc}{dk}.$$

If the group velocity is actually greater than the phase velocity, the fact is named by anti-dispersion. From Fig. 5, it is obvious that the anti-dispersion appears in the all modes of Love waves with the piezoelectric constant variation. In other words, the rate of the energy propagation exceeds that of the wave propagation. Therefore, it is illustrated that waves will appear to originate at the rear of the group, travel to the front and disappear (Julius, 1978). Note that, the anti-dispersion also occur in the cases of the dielectric constant variation.

For $\xi = 0.001$, the first mode of Love waves has two kinds of the phase velocity corresponding to one wave number in the certain wave number range, which can be seen in Fig. 2c. Combining with Fig. 6, it can be found that the first mode has both the dispersion and anti-dispersion. Therefore, it is possible that energy propagation does not concentrates in the same direction, and a part of energy propagates in dispersion behaviors, other part of energy in anti-dispersion behaviors. Simultaneously, negative group velocities are seen for the certain wave number range in Fig. 6. It means that the direction in which the energy propagates

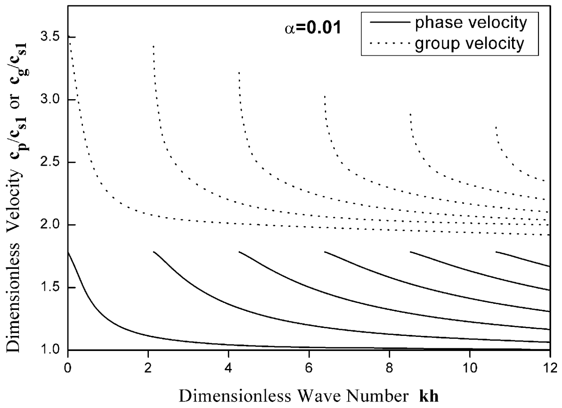

Fig. 5. The dimensionless phase velocity and dimensionless group velocity.

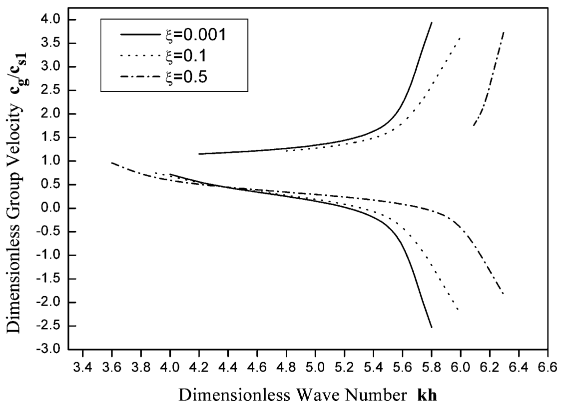

Fig. 6. The dimensionless group velocity in the case of the elastic gradient variation.

is opposite to that of the wave propagation. This fact indicates that the wave propagates in the positive direction of y-axis, but the group travels in the negative direction. The same phenomenon has been observed in not only an isotropic plate (Lysmer, 1970) but also a hybrid composite laminated plate (Liu et al., 1991b). Although the above comments are derived from the first mode, they are also applicable to other modes.

6.2. Effect of gradient variation on the coupled electromechanical factor

The coupled electromechanical factor is an important parameter for designing acoustic sensors. And the coupled electromechanical factor of the mth mode is defined as (Bernhard and Michael, 1997)

$$\kappa_{pm}^2 = \frac{2|c_{pm(\text{open})} - c_{pm(\text{short})}|}{c_{pm(\text{open})}},$$

where $c_{pm(\text{open})}$ and $c_{pm(\text{short})}$ are phase velocities of m th mode, respectively, for the electric open and short cases.

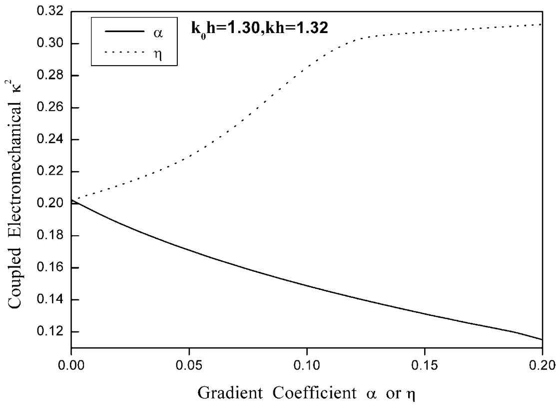

Fig. 7. The Coupled electromechanical factor of the fundamental mode.

Fig. 7 show the relation between the gradient coefficients and the coupled electromechanical factor. It can be seen that the coupled electromechanical factor may be improved by augmenting the gradient of the dielectric constant. It means that the interaction between electrics and mechanics is enhanced in FGPM. For the certain operating frequency of SAW devices of FGPM, as the dielectric gradient increases, the capability of SAW devices can be improved.

6.3. Effect of gradient variation on the cutoff frequency

From Table 3, it can be found that the cutoff frequency of each mode in the homogeneous system is smaller than that of FGPM structure, while the piezoelectric constant varies. However, the cutoff frequency of each mode in the homogeneous system is greater than that of the functionally gradient structure, while the dielectric constant varies. Therefore, the work frequency range of SAW devices is extended by using FGPM with dielectric constant variation.

From Table 4, it can be seen that the cutoff frequency of each mode decreases with the elastic constant gradient increasing. In Tables 3 and 4, the cutoff frequency for the electric short case is less than that of the

Table 3
The cutoff frequencies of the first five modes ($\alpha = 0.01, \eta = 0.01$)

Materials	Mode				
	1st $\times 10^6$ Hz	2nd $\times 10^6$ Hz	3rd $\times 10^6$ Hz	4th $\times 10^6$ Hz	5th $\times 10^6$ Hz
Homogeneous piezoelectric layer					
Open	1.4968516	2.9938514	4.4908512	5.9878510	7.4848508
Short	1.4011251	2.8947212	4.3916672	5.8886618	7.3856615
FGPM layer					
e_{15}					
Open	1.4969446	2.9945435	4.4929567	5.9922626	7.4923953
Short	1.4011421	2.8950702	4.3930648	5.8920073	7.3918177
ε_{11}					
Open	1.4959714	2.9910703	4.4856286	5.9798624	7.4738851
Short	1.4007325	2.8927032	4.3873594	5.8816857	7.3757758

Table 4
The cutoff frequencies of the first four modes with the elastic constant variation

Gradient	Mode			
	1st × 10^6 Hz	2nd × 10^6 Hz	3rd × 10^6 Hz	4th × 10^6 Hz
$\xi = 0.01$				
Open	2.592680621	5.185617847	7.778555080	10.37149232
Short	2.420873818	5.013498937	7.606436337	10.19937411
$\xi = 0.1$				
Open	2.559905738	5.120077250	7.680246220	10.24041456
Short	2.387386780	4.947243077	7.507422033	10.06759579
$\xi = 0.5$				
Open	2.415927850	4.822488860	7.250741167	9.667916343
Short	2.239571389	4.656985237	7.074300313	9.491505967
$\xi = 1.0$				
Open	2.249085820	4.505907840	6.761058857	9.015793427
Short	2.068785205	4.325311763	6.580614830	8.835417607
$\xi = 2.0$				
Open	1.985005681	4.000357677	6.008945627	8.015866653
Short	1.801674142	3.816950143	5.825914607	7.832985520

electric open case no matter how the material constants vary. So SAW devices generally work in the electric short case on the free surface.

7. Conclusions and discussions

From the numerical examples, the following conclusions can be drawn:

- The dispersion of Love waves in the FGPM layer results from both geometrical and physical dispersion. The geometrical dispersion is caused by the thickness of the guiding layer, and thereby the material constant variation leads to the physical dispersion. Furthermore, the anti-dispersion is a universal phenomenon which occurs in the inhomogeneous material.
- The coupled electromechanical factor of Love waves in FGPM structure increases, as the gradient coefficient of the dielectric constant is increased. And the dielectric constant gradient is within $(0, 0.12)$, the coupled electro-mechanical factor has a remarkable increase.
- For the piezoelectric and elastic constants variation, the cutoff frequency of Love wave in FGPM structure is greater than that of the homogeneous structure. However, the cutoff frequency of Love wave in FGPM structure is smaller in the dielectric constant variation.

The above conclusions are very applicable and can be expected to be utilized in design of SAW devices. Some results are also applied to detect the material properties of the manufactured FGPMs.

The present work introduces a assumption that the variations of material constants are independent through the thickness. Although there are differences between this assumption and reality of real FGPM, the individual effects of different material constant on dispersion behaviors can be revealed by this assumption. But the further studies of investigating real FGPM are needed.

Acknowledgement

This work was supported by the National Science Foundation of China.

Appendix A. Analytical solution of the ordinary differential equation

The analytical solution of the first ordinary differential equation in Eq. (17) is given by

$$X_1(x) = C_1 \mathrm{e}^{(\alpha Q_e x)/h} \cdot F\left(1 + \frac{Q_e}{2} - \frac{kh}{2\alpha}, 1 + \frac{Q_e}{2} + \frac{kh}{2\alpha}; 1 + Q_e; Z_e(x)\right) p_e(x) + C_2 \mathrm{e}^{-(\alpha Q_e x)/h} \times F\left(1 - \frac{Q_e}{2} - \frac{kh}{2\alpha}, 1 - \frac{Q_e}{2} + \frac{kh}{2\alpha}; 1 - Q_e; Z_e(x)\right) p_e(x), \tag{A.1}$$

where

$$Q_e = \frac{\sqrt{c_{44}^0 (c_{44}^0 k^2 - \rho_1 c^2 k_0^2)} h}{\alpha c_{44}^0}, Z_e(x) = -\frac{e_{15}(x)}{\beta}.$$

The solution of the corresponding equation in the dielectric constant gradient variation is also expressed by

$$X_1(x) = C_1 \mathrm{e}^{kx} \cdot F\left(1 - Q_\varepsilon + \frac{kh}{\eta}, 1 + Q_\varepsilon + \frac{kh}{\eta}; 1 + \frac{2kh}{\eta}; Z_\varepsilon(x)\right) p_\varepsilon(x) + C_2 \mathrm{e}^{-kx} \times F\left(1 - Q_\varepsilon - \frac{kh}{\eta}, 1 + Q_\varepsilon - \frac{kh}{\eta}; 1 - \frac{2kh}{\eta}; Z_\varepsilon(x)\right) p_\varepsilon(x), \tag{A.2}$$

where

$$Q_\varepsilon = 3 + \frac{\sqrt{c_{44}^0 (c_{44}^0 k^2 - \rho_1 c^2 k_0^2)} h}{\eta c_{44}^0}, \quad Z_\varepsilon(x) = -\frac{c_{44}^0 \varepsilon_{11}(x)}{(e_{15}^0)^2}.$$

The functions $F(\bullet, \bullet; \bullet; \bullet)$ in Eqs. (A.1) and (A.2) are the hypergeometric functions.

References

Bernhard, J., Michael, J.V., 1997. Properties of Love waves: applications in sensors. Smart Materials and Structures 6, 668–679.

Ghatak, A.K., Gallawa, R.L., Goyal, I.C., 1991. Modified airy function an WKB solutions to the wave equation. US Government Printing Office, Washington, DC.

Han, X., Liu, G.R., 2003. Elastic waves propagating in a functionally graded piezoelectric cylinder. Smart Materials and Structures 12 (6), 962–971.

Han, X., Liu, G.R., Lam, K.Y., Ohyoshi, T., 2000. A quadratic element for analyzing stress waves in functionally graded materials and its applications for material characterization. Journal of Sound and Vibration 236 (2), 307–321.

Han, X., Liu, G.R., Xi, Z.C., Lam, K.Y., 2001. Transient waves in a functionally graded cylinder. International Journal of Solids and Structures Vol. 38, 3021–3037.

Han, X., Liu, G.R., Xi, Z.C., Lam, K.Y., 2002. Characteristics of waves in a functionally graded cylinder. International Journal for Numerical Methods in Engineering 53 (3), 653–676.

Julius, M., 1978. The Theory of Elastic Waves and Waveguides. North-Holland Publishing Company, Amsterdam, New York.

Karl, F.G.., 1975. Wave Motion in Elastic Solids. Clarendon Press, Oxford.

Kawasaki, A., Watanabe, R., 1997. Concept and P/M fabrication of functionally gradient materials. Ceramics International 23, 73–83.

Liu, G.R., Tani, J., 1991. Characteristic of wave propagation in functionally gradient piezoelectric material plates and its response analysis. Part 1: theory; Part 2: calculation results. Transactions of the Japan Society of Mechanical Engineers 57A (541), 2122–2133.

Liu, G.R., Tani, J., 1992. SH surface waves in functionally gradient piezoelectric material plates. Transactions of the Japan Society of Mechanical Engineers 58A (547), 504–507.

Liu, G.R., Tani, J., 1994. Surface waves in functionally gradient piezoelectric plates. Transactions of the American Society of Mechanical Engineers Vol. 116, 440–448.

Liu, G.R., Tani, J., Ohyoshi, T., 1991a. Lamb waves in a functionally gradient material plates and its transient response. Part 1: Theory; Part 2: Calculation results. Transaction of the Japan Society of Mechanical Engineers 57 (535), 131–142.

Liu, G.R., Tani, J., Ohyoshi, T., Watanabe, K., 1991b. Characteristic wave surface in anisotropic laminated plates. Journal of Vibration and Acoustics Vol. 113, 279–285.

Liu, H., Wang, Z.K., Wang, T.J., 2001. Effect of initial stress on the propagation behavior of Love waves in a layered piezoelectric structure. International Journal of Solids and Structures 38, 37–51.

Liu, G..R., Dai, K.Y., Han, X., Ohyoshi, T., 2003. Dispersion and characteristics of waves in functionally graded piezoelectric plates. Journal of Sound and Vibration 268, 131–147.

Liu, G.R., Han, X., Lam, K.Y., 1999. Stress waves in functionally gradient materials and its use for material characterization. Composites Part B: Engineering 30, 383–394.

Lysmer, J., 1970. Lumped mass method for Rayleigh waves. Bulletin of the Seismological Society of America 60 (1), 89–104.

Nanny, F., Per Olof, F., 2002. Physical Problems Solved by the Phase-Integral method. Cambridge University Press, Cambridge.

Ohyoshi, T., 1993. New stacking layer elements for analyses of reflection and transmission of elastic waves to inhomogeneous layers. Mechanics Research Communication 20 (4), 353–359.

Ohyoshi, T., 1995. Linearly inhomogeneous layer element for reflectance evaluation of inhomogeneous layers. Dynamic Response Behavior Composition 46, 121–126.

Ohyoshi, T., Sui, G.J., Miuro, K., 1996. Using of stacking model of the linearly inhomogeneous layers elements. Proceedings of the ASME Aerospace Division 52, 101–106.

Pauley, K.E., Dong, S.B., 1976. Analysis of plane waves in laminated piezoelectric plates. Wave Electronics 1, 265–285.

Shiosai, T., Mikamura, Y., Takeda, F., Kwabata, A., 1986. High-coupling and high-velocity SAW using ZnO and AIN Films on a glass subrate. IEEE Transactions on UFFC 33 (3), 324–330.

Siao, J.C.T., Dong, S.B., 1994. Frequency spectra of laminated piezoelectric cylinders. ASME Journal of Vibration and Acoustics 116, 364–370.

Ueda, S., 2003. Crack in functionally graded piezoelectric strip bonded to elastic surface layers under electromechanical loading. Theoretical and Applied Fracture Mechanics 40, 225–236.

Wang, B.L., 2003. A mode III crack in functionally graded piezoelectric materials. Mechanics Research Communication 30, 151–159.

Wang, Q., Quek, S.T., 2001. Love waves in piezoelectric coupled solid media. Smart Materials and Structures 10, 380–388.